11248 *J. Phys. Chem. A* **2000,** *104,* 11248−11256

Syntheses of NCN and NC_3N from Ionic Precursors in the Gas Phase and an Unusual Rearrangement of Neutral NC_3N: A Joint Experimental and Theoretical Study

Stephen J. Blanksby, Suresh Dua, and John H. Bowie*

Department of Chemistry, The University of Adelaide, South Australia 5005, Australia

Detlef Schröder and Helmut Schwarz*

Institut für Organische Chemie, Technische Universität Berlin, Strasse des 17. Juni 135,
D-10623 Berlin, Germany

Received: April 25, 2000; In Final Form: July 20, 2000

Neutral NCN is made in a mass spectrometer by charge stripping of $NCN^{-\bullet}$, while neutral dicyanocarbene NCCCN can be formed by neutralization of either the corresponding anionic and cationic species, $NCCCN^{-\bullet}$ and $NCCCN^{+\bullet}$. Theoretical calculations at the RCCSD(T)/aug-cc-pVTZ//B3LYP/6-31+G(d) level of theory indicate that the $^3\Sigma_g^-$ state of NCCCN is 18 kcal mol^{-1} more stable than the $^1A_1$ state. While the majority of neutrals formed from either $NCCCN^{-\bullet}$ or $NCCCN^{+\bullet}$ correspond to NCCCN, a proportion of the neutral NCCCN molecules have sufficient excess energy to effect rearrangement, as evidenced by a loss of atomic carbon in the neutralization reionization (NR) spectra of either $NCCCN^{+\bullet}$ and $NCCCN^{-\bullet}$. ^{13}C labeling studies indicate that loss of carbon occurs statistically following or accompanied by scrambling of all three carbon atoms. A theoretical study at the B3LYP/6-31+G(d)//B3LYP/6-31+G(d) level of theory indicates that C loss is a consequence of the rearrangement sequence NCCCN → CNCCN → CNCNC and that C scrambling occurs within singlet CNCCN via the intermediacy of a four-membered C_{2v}-symmetrical transition structure.

Introduction

Small, unsaturated molecules are of much interest to chemists and astrophysicists. For example, the interstellar heterocumulenes C_3O, C_3S and C_3N have been studied experimentally and theoretically.[1−3] Diheterocumulenes of the general formula XC_3Y have also been studied, but none have, to date, been detected in interstellar or circumstellar dust clouds.[4] Carbon suboxide (OC_3O) is relatively stable,[5] while NC_3O has been observed during a neutralization/reionization experiment in a mass spectrometer.[6] The transient dicyanocarbene NC_3N is accessible by photolysis or pyrolysis of dicyanodiazomethane,[7] inserts rapidly into aliphatic C−H bonds, and adds across C=C bonds.[8] Electron spin-resonance shows the ground state of NC_3N to be a triplet.[9] Similar trends have been observed for the analogue NCN. This species is made photolytically or pyrolytically from cyanogen azide (NCN_3), and it also inserts into C−H bonds.[10,11] The ground state is a linear triplet, as shown by electron spin resonance spectroscopy.[9]

A number of other studies of NCN and NCCCN have been reported. Infrared absorptions of NCCCN trapped in a low-temperature matrix have been measured.[12,13] Both laser-induced fluorescence and infrared spectra have been reported for NCN.[14−16] The neutrals NCN and NCCCN have been studied theoretically: a nonlinear $^3B_1$ ground state NCCCN structure was calculated in early studies, and found to be some 17 kcal mol^{-1} more stable than the lowest energy singlet state.[17−19] Recent high level calculations for NCN have found a linear $^3\Sigma_g^-$ ground state with a C−N bond length of 1.233 Å in excellent agreement with the value of 1.231 Å determined experimentally.[20,21]

We have reported the formation of a variety of neutral cumulenes and heterocumulenes by neutralization of anions and/or cations in mass spectrometric devices.[22,23] In this paper, we report the formations of (i) NCN by charge stripping of the precursor $NCN^{-\bullet}$, and (ii) NCCCN by neutralization of both $NCCCN^{+\bullet}$ and $NCCCN^{-\bullet}$. Formation of the two anions has been reported previously in the reactions of cyanamide and malononitrile, respectively, with $O^{-\bullet}$ according to reactions 1 and 2.[24] The ionic product of reaction 1 has been shown to be $NCN^{-\bullet}$, rather than $NNC^{-\bullet}$ or *cyclo*-$CN_2^{-\bullet}$.[24] Further, $NCN^{-\bullet}$ has been probed by photoelectron spectroscopy which revealed an electron affinity (EA) of 2.484 ± 0.006 eV and a triplet ground state for the neutral species;[25] the radical anion $NCCCN^{-\bullet}$ has not been studied theoretically.

$$NCNH_2 + O^{-\bullet} \rightarrow NCN^{-\bullet} + H_2O \qquad (1)$$

$$(NC)_2CH_2 + O^{-\bullet} \rightarrow (NC)_2C^{-\bullet} + H_2O \qquad (2)$$

This paper reports the formation of NCN and NCCCN by neutralization of the corresponding radical anions and/or cations, their behavior at the neutral stage, and an interesting rearrangement of neutral NCCCN to NCCNC. While these species with an odd number of carbon atoms are likely to exists only as transients in more dense media, the corresponding even-numbered cumulenes are known to form stable compounds which can be isolated as bulk materials, i.e., dicyanogen NCCN and dicyano acetylene NCCCCN.

Experimental Section

Mass Spectrometric Experiments. Most experiments were performed with a VG ZAB 2HF two-sector mass spectrometer of BE configuration (B stands for magnetic and E for electric sector), which has been described previously.[26] In summary,

10.1021/jp001590q CCC: $19.00

precursor anions $NCN^{-\bullet}$ and $NCCCN^{-\bullet}$ were prepared in the chemical ionization (CI) source of the mass spectrometer by the reactions of cyanamide and malononitrile with $O^{-\bullet}$ (from N_2O).[24] $NCCCN^{-\bullet}$ was also generated by dissociative electron ionization (EI) of tetracyanoethylene oxide which generally resulted in higher ion currents than the $O^{-\bullet}$ reaction. The repeller voltage was ca. 0 V, and the electron energy 50−100 eV. The ions were accelerated to 7 keV translational energy and mass selected by means of the magnet. For collisional activation experiments,[27] the ions were collided in the field free regions between B and E with helium at 80% transmission (T) of the incident beam; these conditions approximate single-collision conditions.[28]

In neutralization-reionization experiments from anions to cations ($^{-}NR^{+}$),[29] the radical anions were neutralized by high-energy collisions with molecular oxygen (80% T) in the first of the two collision cells located in the field-free region between B and E. Unreacted ions were deflected away from the beam of neutral species by applying a voltage of 300 V on a deflector electrode located between the two collision chambers. Reionization of the neutrals to cations occurred in the second cell by collision with oxygen (80% T). The resulting mass spectra were recorded by scanning E. Charge reversal mass spectra of the anions to cations ($^{-}CR^{+}$)[29−31] were obtained by colliding the ion beam with oxygen (80% T) in the field free region preceding E. Under these conditions, the $^{-}CR^{+}$ process can be treated as a vertical, two-electron oxidation occurring in a single step at a time scale of a few femtoseconds, although some species may undergo multiple collisions. For direct comparison with the $^{-}NR^{+}$ spectra, the $^{-}CR^{+}$ spectra were also recorded under $^{-}NR^{+}$ conditions (i.e., O_2/O_2, each 80% T). Experiments with positive ions were conducted as follows. The $NCCCN^{+\bullet}$ radical cation was formed by EI of tetracyanoethylene oxide. $^{+}NR^{+}$ experiments were carried out in the field-free region between B and E utilizing benzene (80% T) and O_2 (80% T) as the respective neutralization and reionization reagents. The spectra were recorded a minimum of three times in order to establish their reproducibility.

$^{-}NIDD^{+}$ spectra were obtained by subtracting the normalized peak heights of the CR spectra from those of the corresponding $^{-}NR^{+}$ spectra as described earlier.[32,33] Positive differences in the difference spectra indicate products whose formation involve either decomposition or rearrangement of the intermediate neutral species, while decompositions attributed to the ions appear as negative signals.

The spectra of the ^{13}C labeled derivatives of $NCCCN^{-\bullet}$ (recorded and described in Table 5), and the MS^3-type experiments reported in this paper were carried out using a modified VG ZAB/HF/AMD four-sector mass spectrometer of BEBE configuration which has been described in detail previously.[34] For the $^{+}NR^{+}$/CA experiments, (i) ions were accelerated to 8 keV translational energy and mass selected by means of B(1)/E(1) at mass resolutions of $m/\Delta m = 2000-5000$, (ii) $^{+}NR^{+}$ was carried out in the field-free region between E(1) and B(2) utilizing Xe (90% T) and O_2 (80% T) as the respective neutralization and reionization reagents, (iii) the survivor ion was mass selected by B(2), (iv) collisionally activated (CA) with He (50% T) between B(2) and E(2), and (v) the ionic fragments were monitored by scanning E(2). A multiple collision (CA/CA) spectrum of the cation was recorded for comparison under the same experimental conditions, save for earthing of the deflector electrode. The spectra were accumulated and processed with the AMD-Intectra data system; usually 10−50 scans were averaged to improve the signal-to-noise ratio.

SCHEME 1

$$BrCH_2CO_2H + KCN \rightarrow NCCH_2CO_2H + KBr$$

$$NCCH_2CO_2H + C_2H_5OH \rightarrow NCCH_2CO_2C_2H_5 + H_2O$$

$$NCCH_2CO_2C_2H_5 + NH_3 \rightarrow NCCH_2CONH_2 + C_2H_5OH$$

$$NCCH_2CONH_2 \xrightarrow{POCl_3} NCCH_2CN$$

Synthesis of Precursor Molecules. Cyanamide, malononitrile, and tetracyanoethylene oxide are commercially available samples and were used without further purification. The synthetic sequence used to prepare the two labeled malononitriles has been reported.[35] The four steps of the synthesis are summarized in Scheme 1. When $Br^{13}CH_2COOH$ is used in the first step of this sequence, the product is $NC^{13}CH_2CN$. When $K^{13}CN$ is used in the first step, the product is $N^{13}CCH_2CN$. The incorporation of ^{13}C into both precursors is 99% and is completely retained in the labeled products as shown by positive ion mass spectrometry.

Computational Methods. Geometry optimizations were carried out with the Becke3LYP method[36,37] using the 6-31+G(d) basis within the GAUSSIAN 94 suite of programs.[38] Stationary points were characterized as either minima (no imaginary frequencies) or transition structures (one imaginary frequency) by calculation of the frequencies using analytical gradient procedures. The minima connected by a given transition structure were confirmed by intrinsic reaction coordinate (IRC) calculations. The calculated frequencies were scaled by 0.9804[39] and used for zero-point correction for the electronic energies calculated at this and higher levels of theory. More accurate energies for the B3LYP geometries were determined with the RCCSD(T) method,[40−45] using the Dunning aug-cc-pVDZ and aug-cc-pVTZ basis sets[46,47] within the MOLPRO 97.4 package.[48] Calculations involving GAUSSIAN 94 geometry optimization were carried out using the Power Challenge Super Computer at the South Australian Super Computing Centre (Adelaide). The single point energy calculations with MOLPRO 97.4 were carried out with the Power Challenge Super Computer at the Australian National University Super Computing Facility (Canberra).

Results and Discussion

Theoretical studies of NCN Neutral, Anion, and Cation. Thermochemical and geometrical parameters of neutral NCN calculated at different levels of theory are given in Table 1. The hybrid density functional Becke3LYP method using the modest 6-31+G(d) basis set predicts a ground-state triplet ($^3\Sigma_g^-$) for NCN with a C−N bond length of 1.234 Å and an electron affinity of 2.50 eV compared with experimental values of 1.233 Å[20,21,49] and 2.484 eV,[25] respectively. Although the B3LYP method gives excellent agreement with experiment for the NCN geometries and electron affinities, there have been some concerns raised in the literature about using density functional theory to describe the energetics of carbenes and biradicals.[50] The B3LYP energies calculated for triplet and singlet NCN shown in Table 2 substantially overestimate the experimentally measured triplet−singlet state splitting of 1.01 ± 0.01 eV (Table 1).[51] Thus, single-point energy calculations on the B3LYP geometries were performed using the partially restricted open-shell coupled cluster approach, RCCSD(T), and the larger basis sets aug-cc-pVDZ and aug-cc-pVTZ. These data better reproduce the experimental energy (Table 1) giving values of 1.35 and 1.25 eV, respectively. Larger basis sets may further refine

TABLE 1: Physical Properties Calculated for Neutral NCN at Various Levels of Theory and Theoretical and Experimental Data Available in the Literature

level of theory or experiment type	C−N bond length (Å)	electron affinity (eV)	ionization energy (eV)	singlet−triplet splitting (eV)[a]
B3LYP/6-31+G(d)	1.2341	2.50	12.81	1.46
RCCSD(T)/aug-cc-pVDZ//B3LYP/6-31+G(d)		2.23	12.36	1.35
RCCSD(T)/aug-cc-pVTZ//B3LYP/6-31+G(d)		2.42	12.52	1.25
other levels	1.2334[b]	2.52[c]		
experiment	1.2309[d]	2.484 ± 0.006[c]		1.01[e]

[a] The energy separation between the triplet ground state and the excited singlet electronic state. [b] CCSD(T)/TZ2P calculations, ref 49. [c] CBS-QCI/APNO calculations, ref 25. [c] References 20 and 21. [d] Reference 25. [e] Reference 51.

TABLE 2: Results of Theoretical Calculations for Anionic, Neutral, and Cationic NCN

NCN species	electronic state	C−N bond length (Å)	electronic energy (hartrees)	zero-point energy (hartrees)[d]	relative energy (kcal mol^{-1})[e]
NCN$^{-\bullet}$	$^2\Pi_g$	1.2404[a]	−147.59103[a]	0.00922[a]	0.0[a]
			−147.22972[b]		0.0[b]
			−147.34793[c]		0.0[c]
NCN	$^3\Sigma_g^-$	1.2341[a]	−147.49851[a]	0.00842[a]	57.6[a]
			−147.14696[b]		51.4[b]
			−147.25819[c]		55.8[c]
NCN	$^1\Delta_g^-$	1.2312[a]	−147.44571[a]	0.00915[a]	91.2[a]
			−147.09823[b]		82.5[b]
			−147.21279[c]		84.8[c]
NCN$^{+\bullet}$	$^2\Pi_g$	1.2377[a]	−147.02683[a]	0.00844[a]	353.1[a]
			−146.69248[b]		336.6[b]
			−146.79796[c]		344.6[c]

[a] Calculated using B3LYP/6-31+G(d)//B3LYP/6-31+G(d) [b] Calculated using RCCSD(T)/aug-cc-pVDZ//B3LYP/6-31+G(d) [c] Calculated using RCCSD(T)/aug-cc-pVTZ//B3LYP/6-31+G(d) [d] No scaling used. [e] Relative energy includes ZPE corrected by 0.9804, ref 39.

this value, but these are too expensive of computing time to be used for the larger NC$_3$N species described later in this paper. On the basis of these data, the B3LYP/6-31+G(d) level of theory has been employed for geometry optimizations and calculation of relative energies within a given spin state throughout the paper. However in instances where the energies of different spin states are to be compared, single-point energy calculations have been performed at the RCCSD(T)/aug-cc-pVDZ and RCCSD(T)/aug-cc-pVTZ levels.

The results of calculations for neutral NCN, together with those for the anion and cation, are listed in Table 2. The B3LYP/6-31+G(d) method predicts $D_{\infty h}$ geometry for the neutral, anion and, cation. The $^2\Pi_g$ anion and cation ground states are calculated to have CN bond distances of 1.240 and 1.238 Å, respectively. In valence bond terms, the theoretical data suggest the bonding mnemonics shown in Scheme 2 for ground-state neutral, anion, and cation. The linear geometries and short CN bonds indicate resonance hybrids of cyano-nitrene and allenic contributing structures.

The similar geometries of neutral, anionic, and cationic NCN suggest favorable Franck−Condon factors for vertical electronic transitions between (i) anion and cation ($^-$CR$^+$), (ii) anion and neutral as well as neutral and cation ($^-$NR$^+$) potential surfaces.[52,53] These calculations indicate that collisional electron detachment from NCN$^{-\bullet}$ should yield stable NCN and that the structure of this neutral may be probed by its positive ion spectrum in $^-$NR$^+$ experiments.

Theoretical Studies of NCCCN Neutral, Anion, and Cation. The B3LYP calculations predict a linear $^3\Sigma_g^-$ ground state for neutral NCCCN (Figure 1) with CC and CN bond distances of 1.318 and 1.194 Å, respectively (Table 3), in agreement with available experimental data,[9] but in contrast to an earlier theoretical study which suggeted a C_{2v}-symmetrical structure.[17] However, a bent C_{2v} structure is found for the excited singlet $^1A_1$ electronic state for NCCCN. The C−C bonds in the triplet ground state of NCCCN are between triple and double bonds in character and suggest that in terms of valence bond this species can be considered as a hybrid of a cumulenic nitrene and a cyano-acetylene nitrene. By contrast, the excited singlet state of NCCCN is that of a pure disubstituted carbene. These representations are shown in Scheme 3.

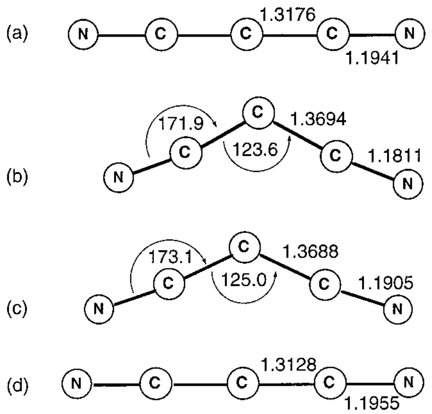

Figure 1. Calculated B3LYP/6-31+G(d) structures of NCCCN for (a) $^3\Sigma_g^-$ ground-state neutral, (b) $^1A_1$ excited-state neutral, (c) $^2B_2$ ground-state anion, and (d) $^2\Pi_u$ ground-state cation.

The data for anionic and cationic NCCCN are shown in Figure 1 and Table 4. In valence bond terms, the charged species may be represented by either addition or removal of an electron from the neutral structures shown in Scheme 3. Since we wish to make neutral NCCCN from anionic and/or cationic precursors, it is of interest to compare the structures of all species shown in Figure 1. Indeed, there exist close structural similarities between (i) NCCCN$^{+\bullet}$ cation and the neutral triplet as well as (ii) NCCCN$^{-\bullet}$ anion and the neutral singlet. The efficiency of vertical oxidation (or reduction) of an incident anion (or cation) can be estimated by calculating the minimum excess energy

SCHEME 2

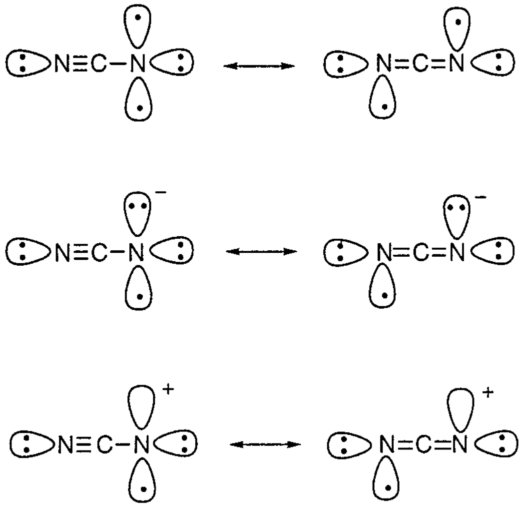

TABLE 3: Physical Properties Calculated for Neutral NCCCN at Various Levels of Theory

level of theory	electron affinity (eV)	ionization energy (eV)	singlet−triplet splitting (eV)[a]
B3LYP/6-31+G(d)	3.07	10.95	0.78
RCCSD(T)/aug-cc-pVDZ//B3LYP/6-31+G(d)	3.11	10.69	0.46
RCCSD(T)/aug-cc-pVTZ//B3LYP/6-31+G(d)	3.20	10.82	0.47

[a] The energy separation between the triplet ground state and the excited singlet electronic state.

SCHEME 3

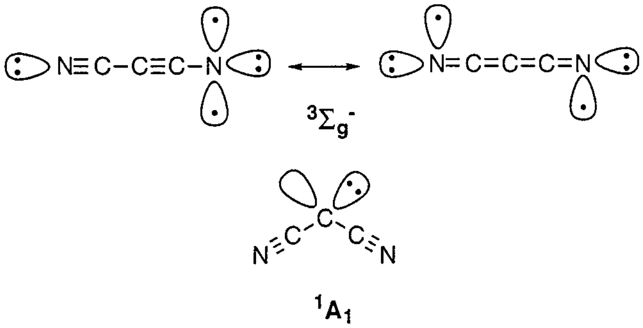

TABLE 4: Results of Theoretical Calculations for Anionic, Neutral, and Cationic NCCCN

NCCCN species	electronic state	electronic energy (hartrees)	zero-point energy (hartrees)[d]	relative energy (kcal mol^{-1})[e]
NCCCN$^{-\bullet}$	$^2B_1$	−223.79962[a]	0.01912[a]	0.0[a]
		−223.23528[b]		0.0[b]
		−223.41429[c]		0.0[c]
NCCCN	$^3\Sigma_g^-$	−223.68708[a]	0.01934[a]	70.8[a]
		−223.12093[b]		71.6[b]
		−223.29674[c]		73.9[c]
NCCCN	$^1A_1$	−223.65783[a]	0.01885[a]	88.8[a]
		−223.10339[b]		82.3[b]
		−223.27897[c]		84.8[c]
NCCCN$^{+\bullet}$	$^2\Pi_u$	−223.28532[a]	0.02010[a]	323.3[a]
		−222.72938[b]		318.1[b]
		−222.89994[c]		323.4[c]

[a] Calculated using B3LYP/6-31+G(d)//B3LYP/6-31+G(d) [b] Calculated using RCCSD(T)/aug-cc-pVDZ//B3LYP/6-31+G(d) [c] Calculated using RCCSD(T)/aug-cc-pVTZ//B3LYP/6-31+G(d) [d] No scaling used. [e] The relative energy includes ZPE corrected by 0.9804, ref 39.

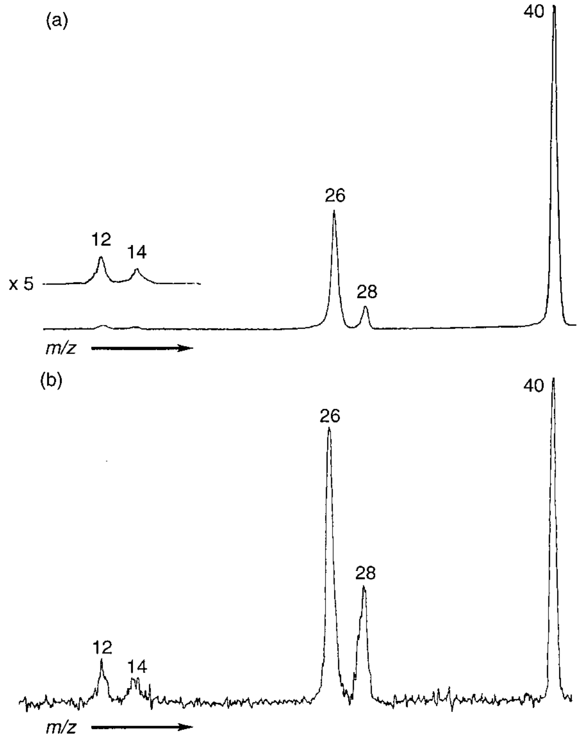

Figure 2. (a) $^-$CR$^+$ (O$_2$, 80% T; O$_2$, 80% T) and (b) $^-$NR$^+$ (O$_2$, 80% T; O$_2$, 80% T) spectra of NCN$^{-\bullet}$.

imparted to the product during the vertical Franck−Condon transition between the two species. For example, the single point energy of the optimized anion geometry on the singlet neutral surface may be calculated and compared with the energy of the optimized minimum on that surface. At the B3LYP/6-31+G(d)//B3LYP/6-31+G(d) level of theory, vertical oxidation of NCCCN$^{-\bullet}$ to the singlet neutral imparts only 0.2 kcal mol^{-1} excess energy to the nascent neutral, while oxidation to the triplet ground-state imparts at least 9.4 kcal mol^{-1}. Conversely, vertical reduction of NCCCN$^{+\bullet}$ to the singlet neutral imparts 5.4 kcal mol^{-1} while reduction to the ground-state triplet imparts almost no excess energy. This suggests that for a $^+$NR$^+$ experiment with NCCCN$^{+\bullet}$, vertical neutralization of the cation radical is likely to preferentially form the triplet ground state of the neutral rather than the singlet. Conversely, in a $^-$NR$^+$ experiment, the excited singlet state should be the predominant neutral product upon vertical electron detachment from the anion. However, since neither of the precursor ions formed in the source is energetically cold, mixtures of singlet and triplet NCCCN neutrals are expected to be formed in the NR experiments. The second step in both NR experiments involves the vertical oxidation of neutral NCCCN to the cation and it is therefore worthwhile to consider the efficiency or otherwise of this electron detachment. Oxidation of the triplet ground state of NCCCN to the doublet cation imparts 2 kcal mol^{-1} excess energy to the nascent cation while the corresponding oxidation of the singlet neutral imparts 11.4 kcal mol^{-1}.

The Formation of NCN. The NCN$^{-\bullet}$ radical anion is formed from cyanamide and O$^{-\bullet}$ according to reaction 1. The structural assignment of this anion is confirmed by the $^-$CR$^+$ spectrum (Figure 2a) which shows loss of atomic nitrogen concomitant with formation of the cyanide cation as the major fragmentation. A peak corresponding to N$_2^{+\bullet}$ does appear in the spectrum, but it is of substantially lower abundance than the CN$^+$ signal. The $^-$NR$^+$ spectrum of NCN$^{-\bullet}$ shows a strong signal due to the reionized parent (Figure 2b) suggesting that neutral NCN is stable for the duration of the NR experiment (ca 10^{-6} s). The $^-$CR$^+$ and $^-$NR$^+$ spectra are similar, (i) confirming that there

SCHEME 4

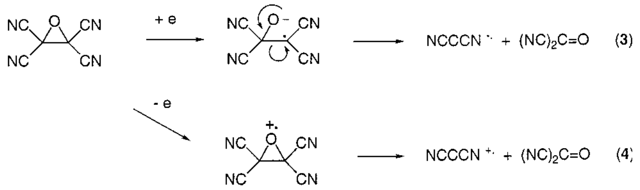

is favorable vertical Franck−Condon overlap between anion, neutral, and cation surfaces as suggested by the theoretical calculations described above, and (ii) indicating that there is no major decomposition or rearrangement that can be ascribed to the transient NCN neutral. The only notable difference between Figures 2a and 2b concerns the ratio of the $N_2^{+\bullet}$ and CN^+ signals which increases from ca. 0.2 in the $^-CR^+$ spectrum to about 0.4 in the $^-NR^+$ experiment. In terms of the NIDD scheme (NIDD = neutral and ion decomposition difference),[32,33] this difference indicates some dissociation of the transient NCN neutral into $C + N_2$. However, we refrain from drawing further conclusions as far as the reactivity of the neutral is concerned because formation of molecular nitrogen is by far the lowest-lying fragmentation pathway, i.e., $\Sigma\Delta H^0_f(C + N_2) = 170$ kcal mol^{-1} compared to $\Sigma\Delta H^0_f(CN + N) = 217$ kcal mol^{-1} and $\Sigma\Delta H^0_f(C + N + N) = 395$ kcal mol^{-1}.[55]

The Formation and Rearrangement of NCCCN. Two methods were used for forming the $NCCCN^{-\bullet}$ anion radical in the mass spectrometer, viz (i) the reaction of malononitrile with $O^{-\bullet}$ (eq 2),[24] and (ii) the dissociative resonance capture of tetracyanoethylene oxide to yield $NCCCN^{-\bullet}$ ($m/z = 64$).[54] The latter process is shown in eq 3 of Scheme 4 and is directly analogous to the photolytic decomposition of cyanoethylene oxides to yield cyanocarbenes.[55] The two anion radicals at $m/z = 64$ formed via reactions 2 and 3 give identical $^-CR^+$ and $^-NR^+$ spectra, and are thus assumed to possess the same structure. As the intensity of $m/z = 64$ is significantly stronger in the tetracyanoethylene oxide spectrum, we have employed reaction 3 in the experiments described further below. The $NCCCN^{+\bullet}$ cation radical is formed following ionization of tetracyanoethlyene oxide according to eq 4. The $^+NR^+$ spectrum of the $NCCCN^{+\bullet}$ cation and the $^-NR^+$ spectrum of the $NCCCN^{-\bullet}$ anion are essentially the same (see later), thus suggesting that the same neutral transients are formed from cationic and anionic precursors.

The $^-CR^+$ spectrum of $NCCCN^{-\bullet}$ (Figure 3a) shows major losses of N and NC consistent with C−N and C−C bond cleavages of an NCCCN backbone. Similarly, the collisional activation mass spectrum of $NCCCN^{+\bullet}$ from tetracyano ethylene oxide (Figure 4a) shows major losses of N and CN, also consistent with structure $NCCCN^{+\bullet}$ for the parent cation radical.

With the connectivity of the anion and cation radicals of NCCCN established, it remains for us to investigate the stability of the corresponding neutrals on the time scale of the NR experiment. The $^-NR^+$ spectrum of $NCCCN^{-\bullet}$ (Figure 3b) and the $^+NR^+$ spectrum of $NCCCN^{+\bullet}$ (Figure 4b) are very similar as far as the fragment ions are concerned. Both show intense peaks corresponding to the parent cation radical formed by the reionization processes; these observations imply the survival of "C_3N_2" neutrals for the period between neutralization and reionization (ca 10^{-6} s). The fact that the relative intensity of the recovery signal is about two times larger in the $^+NR^+$ compared to the $^-NR^+$ experiment is likely to be a consequence of Franck−Condon effects which are operative in collisional electron transfer in the femtosecond time scale.[32,33] However, the possibility that metastable dissociative states of some cations are involved cannot be excluded on available evidence.

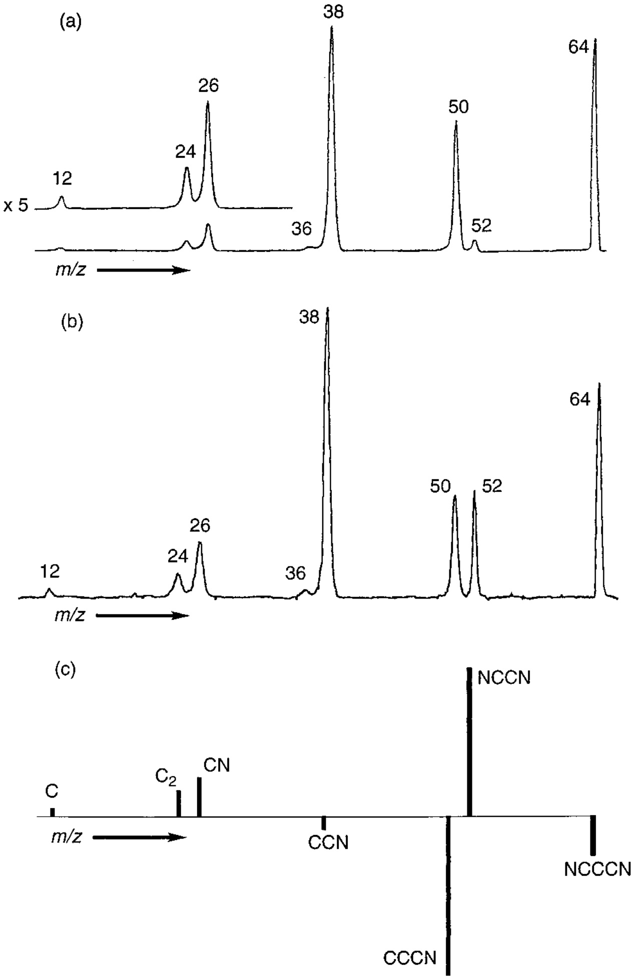

Figure 3. (a) $^-CR^+$ (O_2, 80% T; O_2, 80% T), (b) $^-NR^+$ (O_2, 80% T; O_2, 80% T), and (c) $^-NIDD^+$ spectra of $NCCCN^{-\bullet}$.

Comparison of (i) the $^-CR^+$ and $^-NR^+$ spectra of $NCCCN^{-\bullet}$ (Figure 3a,b) and (ii) the CA and $^+NR^+$ spectra of $NCCCN^{+\bullet}$ (Figure 4a,b) reveals the same important difference in both cases. The NR spectra show significant peaks corresponding to loss of carbon: the corresponding peaks are less abundant in the analogous $^-CR^+$ and CA spectra. Subtraction of the normalized $^-CR^+$ spectrum of $NCCCN^{-\bullet}$ from the $^-NR^+$ spectrum gives the $^-NIDD^+$ spectrum[32,33] shown in Figure 3c. The major feature of the $^-NIDD^+$ spectrum is the positive signal for loss of atomic carbon, indicating fragmentation of a rearranged parent neutral upon reionization: the negative signal for the ion is consistent with the occurrence of a rearrangement at the neutral stage.[32,33] Nevertheless, the intense recovery signals in both NR experiments imply the formation of neutral NCCCN, while the NIDD results imply that a proportion of initially formed neutrals have sufficient energy to rearrange (perhaps to NCCNC or, less likely, to CNCNC) during the lifetime of the neutral transient in the NR experiment.[32,33] Either of these rearranged neutrals could account for the observed loss of C in the NR spectra.

If the rearrangement occurring during neutralization−reionization does involve a nitrile−isonitrile rearrangement, then the determination of which carbon is lost in this process may assist with the elucidation of such a mechanism. To this end, we prepared the two malononitriles shown in Scheme 5 in order to selectively generate the corresponding ^{13}C-labeled anions according to eqs 5 and 6. If the rearranged neutrals generated in

TABLE 5: Fragmentations and Fragment Abundances of the CR, NR, and CA Spectra Recorded for the Two Anion Isotopomers $N^{13}CCCN^{-\bullet}$ and $NC^{13}CCN^{-\bullet}$[a]

precursor ion	spectrum type	fragmentations mass/charge ratio (relative intensity)[b,c]
$N^{13}CCCN^{-\bullet}$	$^-CR^+$	65(100), 53(2), 52(2), 51(15), 39(40), 38(21), 27(1), 26(1), 25(0), 24(1)
	$^-NR^+$	65(100), 53(12), 52(7), 51(16), 39(39), 38(21), 27(6), 26(6), 25(3), 24(2).
	CA (anion)	51(21), 39(7), 38(6), 27(67), 26(100)
$NC^{13}CCN^{-\bullet}$	$^-CR^+$	65(100), 53(4), 52(2), 51(12), 39(49), 38(10), 27(1), 26(6), 25(3), 24(1)
	$^-NR^+$	65(100), 53(9), 52(4), 51(11), 39(44), 38(11), 27(2), 26(7), 25(3), 24(1).
	CA (anion)	51(5), 39(14), 38(1), 27(15), 26(100)

[a] To avoid possible interferences in MS/MS studies using two sectors only, the CR and NR spectra of these isotopomers were recorded with the Berlin instrument using B(1)/E(1) mass selected anions by performing the collision experiments in the field free region preceding B(2) while scanning the positive fragments with B(2). [b] For $^-CR^+$ and $^-NR^+$ intensities are given as percentages of the parent ions, while for CA spectra the values are given as percentage of the base peaks. [c] Because of incompleteness of the isotopic labeling (99 atom % ^{13}C) for both precursors, the mass-selected $N^{13}CCCN^{-\bullet}$ and $NC^{13}CCN^{-\bullet}$ at *m/z* 65 were interfered with by about 10% of the isobaric $(NC)_2CH^-$ anion stemming from unlabeled malonitrile. On the basis of the H atom losses observed experimentally, the intensities given are corrected for this isotopic interference by recording the corresponding spectra of $(NC)_2CH^-$ as references. The spectra of $(NC)_2CH^-$ are as follows: (i) CA (anion), 64 (73), 51(63), 50(31), 39(98), 38(41), 26(100). (ii) $^-CR^+$, 65(100), 64(30), 53(1), 51(11), 50(5), 39(8), 38(20), 27(1), 26(3), 25(2), 24(1). (iii) $^-NR^+$, 65(100), 64(39), 53(1), 51(9), 50(6), 39(9), 38(27), 27(1), 26(2), 25(1), 24(1).

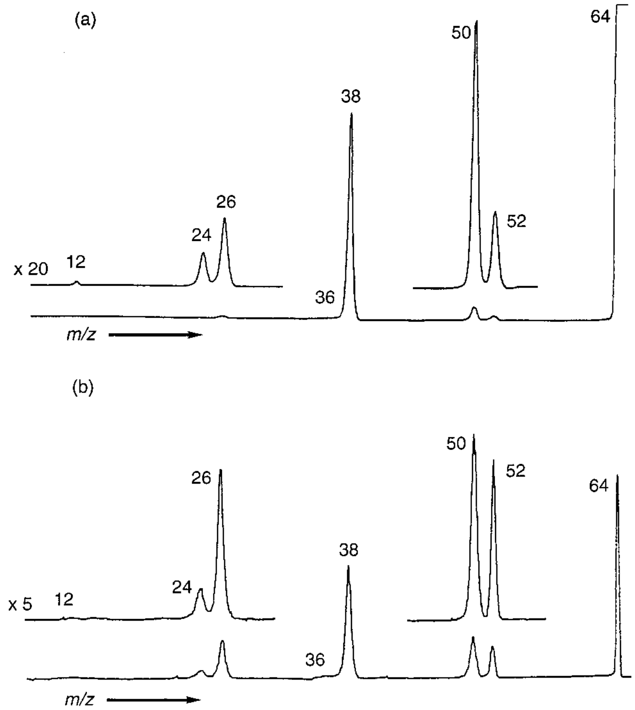

Figure 4. (a) CA (He, 80% T) and (b) $^+NR^+$ (benzene, 70% T; O_2, 80% T) spectra of $NCCCN^{+\bullet}$.

SCHEME 5

$$N^{13}CCH_2CN + O^{-\bullet} \rightarrow N^{13}CCCN^{-\bullet} + H_2O \qquad (5)$$

$$NC^{13}CH_2CN + O^{-\bullet} \rightarrow NC^{13}CCN^{-\bullet} + H_2O \qquad (6)$$

$$N^{13}CCCN \rightarrow {}^{13}CNCCN \text{ and } N^{13}CCNC \qquad (7)$$

$$NC^{13}CCN \rightarrow CN^{13}CCN \qquad (8)$$

reactions 7 and 8 lose carbon only from the two ends of the molecules, then ^{12}C and ^{13}C should be lost in the ratio 1:1 from the neutral products of reaction 7, whereas ^{12}C should be lost exclusively from the product of reaction 8.

The CA, $^-CR^+$, and $^-NR^+$ spectra of $N^{13}CCCN^{-\bullet}$ and $NC^{13}CCN^{-\bullet}$ are reported in Table 5. The most critical observation arising from the $^-NR^+$ spectra of the ^{13}C-labeled anion radicals is that the losses of ^{12}C and ^{13}C occur in an almost statistical manner from each, i.e., the peaks at $m/z = 53$ and 52 appear in ratios close to 2:1. These results are neither in accord with the expected 1:1 ratio of ^{12}C and ^{13}C losses from the products of reaction 7 nor the exclusive loss of ^{12}C from the rearranged product of reaction 8. Instead, these data show that complete carbon-atom scrambling takes place, but do not indicate whether this scrambling occurs at the anion, neutral, or cation stage of the $^-NR^+$ experiment.

The CA spectrum of $NC^{13}CCN^{-\bullet}$ (Table 5) shows predominant loss of ^{13}CCN and formation of CN^-. The small $^{13}CN^-$ fragment (14%) can probably be attributed to collisional activation of the radical anion; the same conclusion can be derived from consideration of the C_2N^- and $^{13}CCN^-$ fragments. The CA spectrum of $N^{13}CCCN^{-\bullet}$ shows losses of $CN/^{13}CN$ and $C_2N/^{13}CCN$ in ratios close to 1:1 (see also footnote to Table 5). In summary, the CA spectra of the labeled radical anions therefore indicate that scrambling of carbons in the anion is, at best, only a minor process.

The $^-NR^+$ spectra (Table 5) of both isotopomers show a statistical distribution of ^{12}C and ^{13}C in the fragments: this is indicative of complete carbon atom scrambling. Therefore, the neutral process (rearrangement or fragmentation) leading to loss of carbon in the $^-NR^+$ spectra occurs concomitant with equilibration of the carbon atoms. It seems reasonable to suggest that a certain population of neutrals which are formed with sufficient internal energy to rearrange may also scramble as part of, or in addition to, rearrangement. A further experiment to substantiate this conclusion would be to compare the results of a $^+NR^+$/CA experiment of $NCCCN^{+\bullet}$ with those of a CA experiment of $NCCCN^{+\bullet}$, i.e., where the parent (recovery) ion in the $^+NR^+$ experiment is collisionally activated in a third collision, and the loss of carbon in the resulting CA spectrum compared with the loss of carbon in the CA spectrum carried out under the same pressure conditions of the $^+NR^+$/CA experiment. The two comparative spectra used for this final experiment are shown in Figure 5. The loss of C is substantially more pronounced in the CA spectrum of the $^+NR^+$ recovery ion than in the multiple collision CA spectrum run under the same conditions. This suggests that the loss of C is due to a rearrangement product of neutral NCCCN, which is then reionized, rather than by a fragmentation exclusively occurring for the neutral species. This result is in line with the available thermochemical data which suggests that the fragmentation, $C_3N_2 \rightarrow C_2N_2 + C$, should be endothermic by 107 kcal mol^{-1}.[55]

The Mechanisms of the Rearrangement and Carbon Scrambling Reactions. What is the mechanism of the rearrangement of NCCCN which causes complete scrambling of the three carbons? Initial rearrangement of NCCCN to the isonitrile CNCCN or even to the diisonitrile CNCNC seems plausible, but this, by itself, does not explain the equilibration of the three carbons. If these rearrangements are indeed operating, there must also be a competitive reaction that is

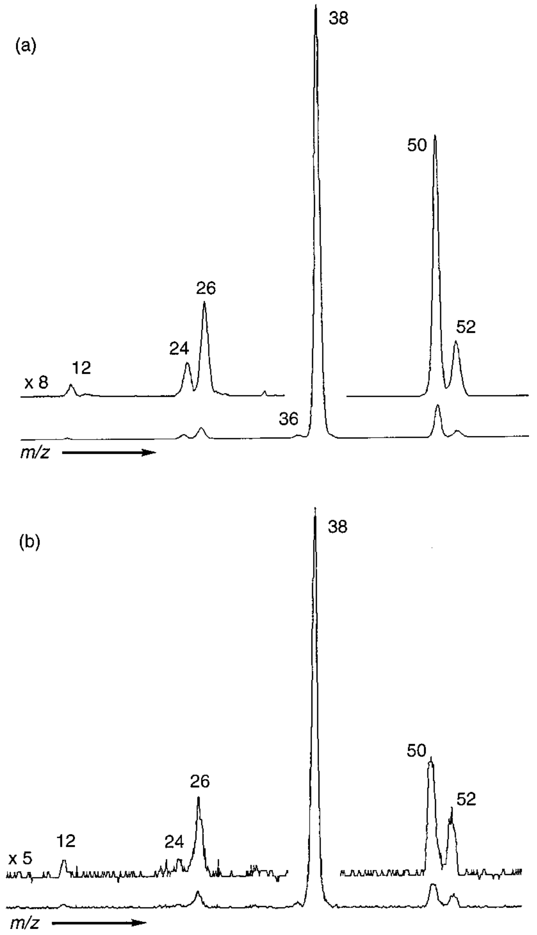

Figure 5. (a) CA/CA (Xe 90% T; O_2, 80% T; He 50% T) and (b) $^+$NR$^+$/CA (Xe 90% T; O_2, 80% T; He 50% T) spectra of NCCCN$^{+\bullet}$.

effecting equilibration of the three carbon atoms. Isonitrile−nitrile rearrangements have been known for more than a 100 years.[56,57] Theoretical and experimental studies have been carried out for this rearrangement.[58,59] The free energy difference between an isonitrile and the more stable nitrile is generally some 15 kcal mol^{-1} and the barrier for the rearrangement is typically 45 kcal mol^{-1}.[60] In contrast, reported examples of the less favorable nitrile−isonitrile rearrangement are rare.[61]

The $^3\Sigma_g^-$ and $^1A_1$ states of NCCCN are separated by 18 kcal mol^{-1} at the B3LYP level of theory[62] although RCCSD(T) single point energy calculations (see earleir discussion) suggest that this energy splitting is closer to 11 kcal mol^{-1} (Tables 3 and 4). Both will be formed during the neutralization process, and thus rearrangement of both states must be considered. We have investigated the rearrangements NCCCN → CNCCN → CNCNC at the B3LYP/6-31+G(d)//B3LYP/6-31+G(d) level of theory for both triplet and singlet reactions. These calculations show that rearrangement of the excited singlet state is energetically more favorable than that of the ground-state triplet. Results of the singlet rearrangement are considered first and are summarized in Figures 6 and 7; electronic and zero-point energies are given in Table 6 while full geometrical data for the stable species and transition structures are available as Supporting Information. The rearrangement of singlet NCCCN (**1**) to the singlet cyano-isocyano carbene CNCCN (**3**) is shown in Figure 6. The isomerization is found to proceed through the intermediacy of a cyclic species (NCC)CN (**2**). The activation energies for the ring-closing and ring-opening steps of this reaction sequence are determined to be 57.8 and 37.3 kcal mol^{-1} respectively. Singlet **3** is a stable minimum some 15 kcal mol^{-1} more energetic than singlet **1**. Further rearrangement of CNCCN (**3**) to CNCNC (**5**) is also possible. This reaction sequence is shown in Figure 7 and is very similar to that shown in Figure 6. The overall reaction is endothermic by 11.9 kcal mol^{-1} with the barriers of the ring closing and ring opening steps being 59.2 and 40.8 kal mol^{-1}, respectively.[63]

Details of the triplet potential surface are summarized in Table 7. The triplet isocyano carbenes CNCCN and CNCNC are substantially less stable than triplet NCCCN by 26 and 51 kcal mol^{-1}, respectively. Accordingly, the nitrile-isonitrile rearrangements are significantly more endothermic for the triplet compared to the singlet species. In addition, the triplet cyclic intermediates are also unstable. For example, triplet **2** is 55 kcal mol^{-1} above the global minimum. Considering that the corresponding minima are already quite energy demanding, these data suggest that isomerism of triplet NCCCN is unlikely on energetic grounds, and we have therefore not considered this possibility further.

We propose that carbon equilibration occurs by the process shown in Scheme 6. The barrier from singlet CNCCN to the C_{2v}-symmetrical transition structure **TS3/3** is calculated to be 36.7 kcal mol^{-1} at the B3LYP/6-31+G(d)//B3LYP/6-31+G(d) level of theory. This barrier may be surmounted since singlet CNCCN is formed from singlet NCCCN with an excess energy of 57.8 kcal mol^{-1} (see Figure 6).[64] Carbon scrambling for the analogous di-isocyano carbene, can, in principle, occur by a process directly analogous to that shown in Scheme 6. The activation barrier for this process is more demanding than that

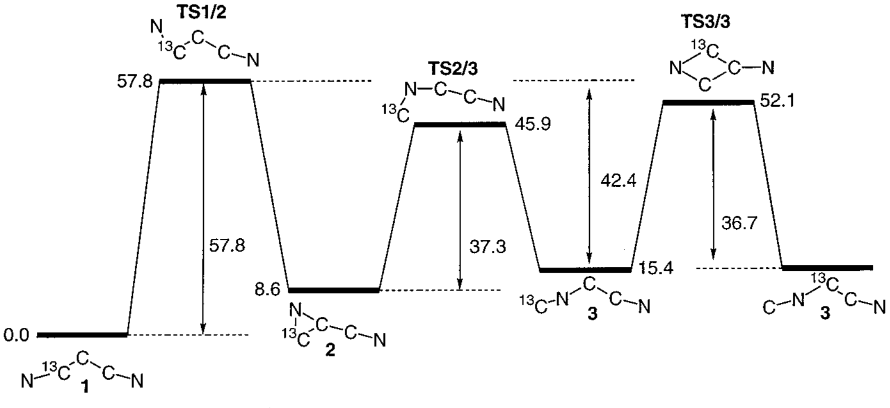

Figure 6. Reaction coordinate diagram (in kcal mol^{-1}) for the rearrangement of singlet neutral NCCCN (**1**) to CNCCN (**3**) and subsequent carbon scrambling. All energies were calculated at the B3LYP/6-31+G(d)//B3LYP/6-31+G(d) level of theory and are given relative to NCCCN with exception of activation energies which are indicated by vertical arrows. The geometries and electronic energies of minima and transition states are given as Supporting Information.

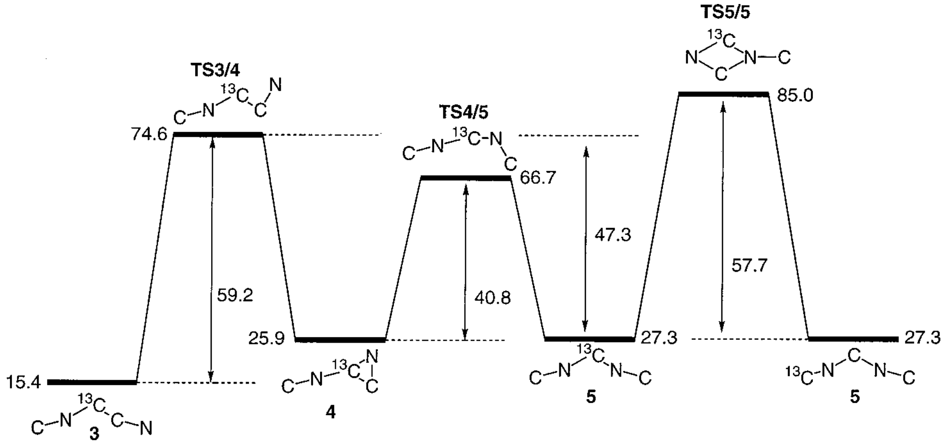

Figure 7. Reaction coordinate diagram (in kcal mol^{-1}) for the rearrangement of singlet neutral CNCCN (**3**) to CNCNC (**5**) and subsequent carbon scrambling. All energies were calculated at the B3LYP/6-31+G(d)//B3LYP/6-31+G(d) level of theory and are given relative to NCCCN with exception of activation energies which are indicated by vertical arrows. The geometries and electronic energies of minima and transition states are given as Supporting Information.

TABLE 6: Energies and Relative Energies of the Singlet Neutral C_3N_2 Isomers and Pertinent Transition States Shown in Figures 6 and 7[a]

C_3N_2 species	electronic state	electronic energy (hartrees)	zero-point energy (hartrees)[b]	relative energy (kcal mol^{-1})[c]
1 [NCCCN]	$^1A_1$	−223.65783	0.01885	0.0
TS1/2	singlet	−223.56382	0.01688	57.8
2 [(NCC)CN]	$^1A'$	−223.64491	0.01964	8.6
TS2/3	singlet	−223.58223	0.01638	45.9
3 [CNCCN]	$^1A'$	−223.63286	0.01842	15.4
TS3/4	singlet	−223.53633	0.01613	74.6
4 [CN(CCN)]	$^1A'$	−223.61706	0.01930	25.9
TS4/5	singlet	−223.54882	0.01607	66.7
5 [CNCNC]	$^1A_1$	−223.61338	0.01792	27.3
TS3/3	singlet	−223.57234	0.01634	52.1
TS5/5	singlet	−223.51852	0.01489	85.0
^1C + NCCN	singlet	−223.44712	0.01652	130.8
$^1C_3 + N_2$	singlet	−223.58567	0.01417	60.5

[a] These are calculated at the B3LYP/6-31+G(d)//B3LYP/6-31+G(d) level of theory. The geometries of these structures are given as Supporting Information. (Table 8). [b] ZPE uncorrected [c] Relative energy includes ZPE corrected by 0.9804, ref 39.

TABLE 7: Energies and Relative Energies of Some of the Triplet Neutral C_3N_2 Isomers Calculated at the B3LYP/6-31+G(d)//B3LYP/6-31+G(d) Level of Theory[a]

C_3N_2 species[a]	electronic state	electronic energy (hartrees)	zero-point energy (hartrees)[b]	relative energy (kcal mol^{-1})[c]
1 [NCCCN]	$^3\Sigma_g^-$	−223.68708	0.01934	0.0
2 [(NCC)CN]	triplet	−223.59678	0.01728	55.4
3 [CNCCN]	$^3A''$	−223.64415	0.01793	26.0
5 [CNCNC]	$^3A''$	−223.60491	0.01802	50.7
^3C + ^{1}NCCN	triplet	−223.51343	0.01652	107.2
$^3C_3 + N_2$	triplet	−223.50526	0.01169	109.4

[a] The geometries of these structures are given as Supporting Information (Table 9). [b] ZPE uncorrected [c] Relative energy includes ZPE corrected by 0.9804, ref 39.

calculated for the process shown in Scheme 6. The transition structure (**TS5/5**) is some 58 kcal mol^{-1} above that of singlet CNCNC and 85 kcal mol^{-1} above the singlet NCCCN global minimum (Figure 7).

Full geometrical details for transition structures **3/3** and **5/5** are available in Supporting Information. Significantly, the cyano-isocyano rearrangement **1** → **3** rearrangement and subsequent carbon scrambling processes on the singlet potential surface is less energetically demanding than even the lowest energy fragmentation channel. We calculate the least endothermic decomposition to be, NCCCN → $C_3 + N_2$, which is endothermic by 60.5 kcal mol^{-1} (Table 6) and notably detection of these fragments in the various NR spectra is negligible (Figures 3-5).

SCHEME 6

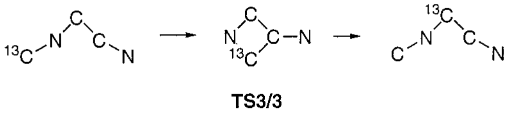

In conclusion, (i) neutral NCN can be formed by collisional electron detachment of NCN$^{-•}$ anion radical, and (ii) neutral NCCCN is accessible via neutralization of either NCCCN$^{+•}$ or NCCCN$^{-•}$ in high-energy collisions. Some of the NCCCN neutrals are formed with excess energy sufficient to effect rearrangement of NCCCN and to cause equilibration of the three C atoms. It is proposed that the rearrangement involves the singlet rearrangement of NCCCN to CNCCN and that the energetically hot CNCCN undergoes a ring closure followed by ring opening which effectively scrambles all three carbons.

Acknowledgment. This project was supported with the aid of a grant from the Australian Research Council. S.D. thanks the ARC for a research associateship. S.J.B. acknowledges the award of a Australian Postgraduate Award and also thanks the Deutscher Akademischer Austauschdienst (DAAD) for financial support. D.S. and H.S. appreciate continuous support by the Deutsche Forschungsgemeinschaft, the Volkswagen-Stiftung, the Fonds der Chemischen Industrie, and the Gesellschaft der Freunde der Technischen Universität Berlin.

Supporting Information Available: Table 8 of geometries of minima and transition structures on the singlet C_3N_2 potential surface. Table 9 of geometries of minima on the triplet C_3N_2 potential surface. This material is available free of charge via the Internet at http://pubs.acs.org.

References and Notes

(1) Brown, R. D.; Eastwood, F. W.; Elmes, P. S.; Godfrey, P. *J. Am. Chem. Soc.* **1983**, *105*, 6496.

(2) Brown, R. D.; Pullin, D. E.; Rice, E. H. N.; Rodler, M. *J. Am. Chem. Soc.* **1985**, *107*, 7877.

(3) Hiratam, Y.; Ohshima, Y.; Endo, Y. *J. Chem. Phys.* **1994**, *101*, 7342. Kasai, Y.; Sumiyoshi, Y.; Endo, Y.; Kawaguchi, K. *Astrophys. J.* **1997**, *477*, L65.

(4) Linear symmetrical XC_3X species do not possess permanent dipole moments, so radioastronomical detection is difficult. However, infrared or other spectroscopic investigations may yet establish the presence of such species in interstellar and circumstellar clouds.

(5) Kappe, T. Zeigler, E. *Angew. Chem., Int. Ed. Engl.* **1974**, *13*, 491.

(6) Muedas, C. A.; Sülzle, D.; Schwarz, H. *Int. J. Mass Spectrom. Ion Processes* **1992**, *28*, 1161.

(7) Ciganek, E. *J. Am. Chem. Soc.* **1965**, *87*, 652.

(8) Ciganek, E. *J. Am. Chem. Soc.* **1966**, *88*, 1979.

(9) Wasserman, E.; Barash, L.; Yager, W. A. *J. Am. Chem. Soc*. **1965**, *87*, 2076.

(10) Anastassiou, A. G.; Simmons, H. E. *J. Am. Chem. Soc.* **1967**, *89*, 3177.

(11) Anastassiou, A. G. *J. Am. Chem. Soc.* **1967**, *89*, 3184.

(12) Smith, W. M.; Leroi, G. E. *Spectrochim. Acta* **1969**, *25A*, 1917.

(13) Dunkin, I. R.; McLuskey, A. *Spectrochim. Acta* **1994**, *50A*, 209.

(14) Jennings, K. R.; Linnett, J. W. *Trans. Faraday Soc*. **1960**, *56*, 1737.

(15) Smith, G. P.; Copeland, R. A.; Crosley, D. R. *J. Chem. Phys.* **1989**, *91*, 1987.

(16) McNaughton, D.; Metha, G.; Tay, R. *Chem. Phys.* **1995**, *198*, 107.

(17) Lucchese, R. R.; Schaefer, H. F. *J. Am. Chem. Soc*. **1977**, *99*, 13.

(18) Baird, N. C.; Taylor, K. F. *J. Am. Chem. Soc.* **1978**, *100*, 1333.

(19) Mueller, P. H.; Rondan, N. G.; Houk, K. N.; Harrison, J. F.; Hooper, D.; Willen, B. H.; Liebman, J. F. *J. Am. Chem. Soc.* **1981**, *103*, 5049.

(20) Herzberg, G.; Travis, D. N. *Can. J. Phys.* **1964**, *42*, 1658.

(21) Beaton, S. A.; Ito, Y.; Brown, J. M. *J. Mol. Spectrosc*. **1996**, *178*, 99.

(22) Selected references: Sülzle, D.; Seemeyer, K.; Schwarz, H.; Witulski, B.; Hopf, H. *Int. J. Mass Spectrom. Ion Processes* **1991**, *105*, Rl. Sülzle, D.; Seemeyer, K.; Witulski, B.; Hopf, H.; Schwarz, H. *Chem. Ber.* **1991**, *124*, 1481. Muedas, C. A.; Sülzle, D.; Schwarz, H. *Int. J. Mass Spectrom. Ion Processes* **1992**, *113*, R17. Muedas, C. A.; Sülzle, D.; Schwarz, H. *Chem. Ber.* **1992**, *125*, 1517. Goldberg, N.; Schwarz, H. *J. Phys. Chem.* **1994**, *98*, 3080. Natterer, J.; Koch, W.; Schröder, D.; Goldberg, N.; Schwarz, H. *Chem. Phys. Lett.* **1994**, *229*, 429. Goldberg, N.; Fiedler, A.; Schwarz, H. *J. Phys. Chem.* **1995**, *99*, 15327. Blanksby, S. J.; Dua, S.; Bowie, J. H.; Schröder, D.; Schwarz, H. *J. Phys. Chem.* **1998**, *102*, 9949. Schröder, D.; Heinemann, C.; Schwarz, H.; Harvey, J. N.; Dua, S.; Blanksby, S. J.; Bowie, J. H. *Chem. Eur. J.* **1998**, *4*, 2550.

(23) Reviews: Sülzle, D.; Schwarz, H. In *Fundamentals of Gas-Phase Ion Chemistry*; Jennings, K. R., Ed.; NATO ASI Series 347; Kluwer: Dordrecht, 1991; p 237. Blanksby, S. J.; Bowie, J. H. *Mass Spectrom Rev.* **1999**, *18*, 131.

(24) Dawson, J. H. J.; Nibbering, N. M. M. *Int. J. Mass Spectrom. Ion Phys.* **1980**, *33*, 3. Kroeker, R. L.; Kass, S. R. *J. Am. Chem. Soc.* **1990**, *112*, 2, 9024.

(25) Clifford, E. P.; Wenthold, P. G.; Lineberger, W. C.; Petersson, G. A.; Ellison, G. B. *J. Phys. Chem.* **1997**, *101*, 4338.

(26) Stringer, M. B.; Bowie, J. H.; Holmes, J. L. *J. Am. Chem. Soc.* **1986**, *108*, 3888.

(27) Busch, K. L.; Glish, G. L.; McLuckey, *Mass Spectrometry/Mass Spectrometry: Techniques and Applications of Tandem Mass Spectrometry*; VCH Publishers: Weinheim, 1988.

(28) Holmes, J. L. *Org. Mass Spectrom.* **1985**, *20*, 169.

(29) McMahon, A. W.; Chowdhury, S. K.; Harrison, A. G. *Org. Mass Spectrom.* **1989**, *24*, 620.

(30) Bowie, J. H.; Blumenthal, T. *J. Am. Chem. Soc.* **1975**, *97*, 2959. Szulejko, J. E.; Bowie, J. H.; Howe, I.; Beynon, J. H. *Int. J. Mass Spectrom. Ion Phys*. **1980**, *34*, 99.

(31) Bursey, M. M. *Mass Spectrom. Rev.* **1990**, *9*, 555.

(32) Hornung, C. A.; Schalley, C. A.; Dieterle, M.; Schröder, D.; Schwarz, H. *Chem. Eur. J.* **1997**, *3*, 1866.

(33) For a review of methods used for the investigation of the reactivity of neutrals by NRMS, see: Schalley, C. A.; Hornung, G.; Schröder, D.; Schwarz, H. *Chem. Soc. Rev.* **1998**, *27*, 91.

(34) Schalley, C. A.; Schröder, D.; Schwarz, H. *Int. J. Mass Spectrom. Ion Processes* **1996**, *153*, 173.

(35) Cheung, H. T. A.; Gray, P. G. *J. Labeled Compd. Radiopharm.* **1983**, *21*, 471.

(36) Becke, A. D. *J. Phys. Chem.* **1993**, *98*, 5648.

(37) Stevens, P. J.; Devlin, F. J.; Chablowski, C. F.; Frisch, M. J. *J. Phys. Chem.* **1994**, *98*, 11623.

(38) Frisch, M. J.; Trucks, G. W.; Schlegel, H. B.; Gill, P. M. W.; Johnson, B. G.; Robb, M. A.; Cheeseman, J. R.; Keith, T.; Peterson, G. A.; Montgomery, J. A.; Raghavachari, K.; Al-Laham, M. A.; Zakrzewski, V. G.; Ortiz, J. V.; Foresman, J. B.; Peng, C. Y.; Ayala, P. Y.; Chen, W.; Wong, M. W.; Andres, J. L.; Replogle, E. S.; Gomperts, R.; Martin, R. L.; Fox, D. J.; Binkley, J. S.; Defrees, D. J.; Baker, J.; Stewart, J. P.; Head-Gordon, M.; Gonzales, C.; Pople, J. A. *GAUSSIAN94*, Revision B, 3rd ed.; GAUSSIAN, Inc.: Pittsburgh, PA, 1995.

(39) Wong, M. W. *Chem. Phys. Lett.* **1996**, *256*, 391.

(40) Cizek, J. *Adv. Chem. Phys.* **1969**, *14*, 35.

(41) Pople, J. A.; Krishnan, R.; Schlegel, H. B.; Binkley, J. S. *Int. J. Quantum Chem.* **1978**, *14*, 545.

(42) Hampel, C.; Peterson, K.; Werner, H.-J. *Chem. Phys. Lett*. **1992**, *190*, 1.

(43) Watts, J. D.; Gauss, J.; Bartlett, R. J. *J. Chem. Phys*. **1993**, *98*, 8718.

(44) Knowles, P. J.; Hampel, C.; Werner, H.-J. *J. Chem. Phys.* **1993**, *99*, 5219.

(45) Deegan, M. J. O.; Knowles, P. J. *Chem. Phys. Lett.* **1994**, *227*, 321.

(46) Dunning, T. H. *J. Chem. Phys.* **1989**, *90*, 1007.

(47) Woon, D. E.; Dunning, J.; T. H. *J. Chem. Phys.* **1993**, *98*, 1358.

(48) Werner, H.-J.; Knowles, P. J.; Almlöf, J.; Amos, R. D.; Deegan, M. J. O.; Elbert, S. T.; Hampel, C.; Meyer, W.; Peterson, K.; Pitzer, R.; Stone, A. J.; Taylor, P. R.; MOLPRO, 97, 4th ed., 1997.

(49) Martin, J. M. L.; Taylor, P. R.; François, J. P.; Gijbels, R. *Chem. Phys. Lett.* **1994**, *226*, 475

(50) Graefenstein, J.; Cremer, D. *Phys. Chem. Chem. Phys*. **2000**, *2*, 2091.

(51) Taylor, T. R.; Bise, R. T.; Asmis, K. R.; Neumark, D. M. *Chem. Phys. Lett.* **1999**, *301*, 413.

(52) Lorquet, J. C.; Leyh-Nihaut, B.; McLafferty, F. W. *Int. J. Mass Spectrom. Ion Processes* **1990**, *100*, 465.

(53) Nguyen, V. G.; Turecek, F. *J. Mass Spectrom.* **1996**, *31*, 842.

(54) Dua, S.; Blanksby, S. J.; Bowie, J. H. *Int. J. Mass Spectrom.* **2000**, *195/196*, 45.

(55) Heats of formation extracted from the NIST database (http:/ webbook.nist.gov): $\Delta H^0{}_f(C_3N_2) = 138$ kcal mol^{-1}, $\Delta H^0{}_f(C_2N_2) = 74$ kcal mol^{-1}, $\Delta H^0{}_f(C) = 170$ kcal mol^{-1}, $\Delta H^0{}_f(C_2N) = 135$ kcal mol^{-1}, $\Delta H^0{}_f$(CN) = 104 kcal mol^{-1}.

(56) Gautier, A. *Ann. Chim. (Paris) Ser. 4.* **1869**, *17*, 215.

(57) Casanova, J. J. In *The Chemistry of the Cyano Group*; Rappoport, Z., Ed.; Interscience: London, 1970; p 885.

(58) Saxe, P.; Yamaguchi, Y.; Pulay, P.; Schaefer III, H. F. *J. Am. Chem. Soc.* **1980**, *102*, 3718.

(59) Meier, M.; Müller, B.; Rüchardt, C. *J. Org. Chem.* **1987**, *52*, 648.

(60) Kohlmaier, G.; Rabinovitch, B. S. *J. Phys. Chem.* **1959**, *63*, 1793.

(61) Booth, M. R.; Frankiss, S. G. *J. Chem. Soc., Chem. Commun.* **1968**, 1347.

(62) For a critical evaluation of DFT approaches in predicting singlet/triplet splitting of carbenes, see: Koch, W.; Holthausen, M. C. *A Chemist's Guide to Density Functional Theory*; Wiley-VCH: Weinheim, 2000; p 168.

(63) A reviewer has asked (i) where this excess energy has come from when our calculations show that the excess energy of the neutral is calculated to be only 9.4 kcal mol^{-1} (as a consequence of the vertical Franck−Condon process), and (ii) is it possible that the rearrangements are occurring from excited electronic states of the neutral? We stress that the Franck−Condon calculation gives the minimum excess energy of the neutral on formation. Two other factors need to be taken into consideration when considering the excess energy range of the neutrals: first, some of the NC_3N anion precursors will have excess energies as a consequence of their mode of formation in the ion source of the mass spectrometer, and second, the various collisions between NC_3N anions and dioxygen in the collision cell will form NC_3N neutrals with a range of excess energies during vertical Franck−Condon processes. Some of these neutrals must have sufficient energy to overcome the initial barrier of 59.2 kcal mol^{-1} (see Figure 6). In answer to the second question, it is certainly possible that upon neutralization, some population of higher electronically states are accessed. As such, it is not possible for us to completely exclude contributions to the rearrangement processes from such species. However, the processes being considered are significant in the NR experiments, suggesting a reasonable proportion of rearranging neutrals. Consequently, the low-lying singlet potential surface seems a more likely candidate. Our calculations provide a plausible pathway for rearrangement and concomitant carbon scrambling (in line with experimental observations) on the singlet neutral potential surface provided that the neutrals are formed with sufficient excess energy.

(64) A reviewer has indicated that symmetrical transition state TS3/3 is an unreasonable structure because it incorporates a "badly bent" CNC ligand. We wish to point out that this transition state is some 37 kcal mol^{-1} above the CNCCN minimum, and that the position of the transition state in the reaction sequence has been confirmed by IRC calculations. In addition, it has been reported that the bent $^2A_1$ state of NCN is calculated to be only 12.78 kcal mol^{-1} less stable than ground-state and linear NCN at the UHF−CCSD(T)/TZ2P level of theory.[49] In addition, the reported[49] geometry of the bent NCN shows significant similarity to that of the NCN portion of the TS3/3 transition state: viz., N−C = 1.3099 Å (1.333 Å in TS3/3), C.-C = 1.6088 Å (1.718 Å in TS3/3) and C−N−C = 75.7° (80.3° in TS3/3).